Available online at www.sciencedirect.com
SCIENCE DIRECT
Journal of Molecular Catalysis A: Chemical 249 (2006) 111–122
JOURNAL OF MOLECULAR CATALYSIS A: CHEMICAL
www.elsevier.com/locate/molcata

Ethylene hydrogenation on $Mo(CO)_6$ derived model catalysts in ultrahigh vacuum: From oxycarbide to carbide to MoAl alloy

Feng Gao, Yilin Wang, W.T. Tysoe *

Department of Chemistry and Biochemistry, Laboratory for Surface Studies, University of Wisconsin-Milwaukee, Milwaukee, WI 53211, USA

Received 6 December 2005; received in revised form 3 January 2006; accepted 3 January 2006
Available online 9 February 2006

Abstract

The ethylene hydrogenation activity is compared for molybdenum oxycarbides, molybdenum carbides and a molybdenum alloy formed by reaction of molybdenum hexacarbonyl with alumina in ultrahigh vacuum using temperature-programmed desorption. It is found that molybdenum oxycarbides are inactive for ethylene hydrogenation. It is shown by forming carbides by reaction between alumina and ethylene that this is due to site blocking by oxygen. The carbide is found to be moderately active for hydrogenation and some ethylene decomposition and self-hydrogenation is also detected. The alloy is found to be the most reactive surface where substantial ethylene hydrogenation and also H–D are detected.

Keywords: Temperature-programmed desorption; Chemisorption; Molybdenum hexacarbonyl; Alumina thin films; Molybdenum carbide; Ethylene; Hydrogenation

1. Introduction

The reaction of molybdenum hexacarbonyl with oxide supports has been used to produce active catalysts [1–12] and in ultrahigh vacuum to synthesize model catalysts supported on planar alumina thin films. In this case, surface-sensitive spectroscopic probes can be used to analyze the surfaces and explore their chemistry [13–16]. $Mo(CO)_6$ reacts with aluminum [17] and dehydroxylated and hydroxylated alumina [18,19] thin films at 700 K to form molybdenum carbide incorporating a small amount of oxygen where low $Mo(CO)_6$ exposures on alumina thin films deposits small molybdenum carbide particles, while higher exposures (∼5000 L of $Mo(CO)_6$) form a thin carbide film that completely covers the surface [18]. Annealing these films to temperatures up to above 1300 K causes CO desorption through alumina reduction by the carbidic carbon, and results in the formation of a thin film of a MoAl alloy [17–19].

It has also been found that, at low $Mo(CO)_6$ exposures, the stoichiometry of the carbide is close to MoC, but gradually changes to Mo_2C with increasing $Mo(CO)_6$ exposure. Molybdenum carbide films formed at 700 K also contain a small amount of oxygen so are referred to in the following as oxycarbides. However, since substrate oxygen can still be detected using Auger and X-ray photoelectron spectroscopies, the oxygen content within the oxycarbide films cannot be precisely determined. Nevertheless, the XPS binding energy of molybdenum in the oxycarbide film is identical to that of pure Mo(1 0 0), suggesting that the oxygen content is rather low. It has been found that, in cases where $Mo(CO)_6$ reacts with thin metallic aluminum films, two mechanisms are responsible for carbide formation. First, deposited molybdenum catalyzes CO dissociation and the resulting oxygen reacts preferentially with aluminum, while carbon reacts with molybdenum to form a carbide. Second, when the aluminum film is completely covered by a reactively formed film, the formation of a continuous carbide layer is due to CO disproportionation, where molecular CO reacts with oxygen originating from CO dissociation to form CO_2, which desorbs, thus depositing additional carbon onto the surface. In cases where aluminum oxide films are used as the supports, CO disproportionation becomes the only reaction pathway for carbide formation. The presence of oxygen in the carbide film (resulting in oxycarbide formation) has been ascribed to the incomplete disproportion of CO. Since oxygen appears to be mobile within the molybdenum carbides [20,21], oxygen appears to reside both on the surface and in the sub-surface regions.

On annealing, the oxycarbide film tends to convert first to pure carbide, due to recombination of O and C atoms *within* the film. TPD experiments using an alumina substrate formed

* Corresponding author. Tel.: +1 414 229 5222; fax: +1 414 229 5036.
E-mail address: wtt@uwm.edu (W.T. Tysoe).

1381-1169/$ – see front matter © 2006 Elsevier B.V. All rights reserved.
doi:10.1016/j.molcata.2006.01.016

with $H_2{}^{18}O$ [18] suggest that this process ceases at ~1300 K so that, above this temperature, the carbide film is oxygen-free. Note, however, that reduction of the alumina substrate is already underway by this temperature. The interaction between the pure carbide and the (partially reduced) alumina substrate releases additional CO to form a MoAl alloy, and this is complete by ~1400 K. The ability to form various carbide, oxycarbide and alloy films on the same surface merely by annealing the oxycarbide films to various temperatures allows the chemistry of these different phases to be compared.

Ethylene hydrogenation has been selected as a model reaction for comparing the reactivity of these phases for two reasons. First, this reaction has been extensively studied and the hydrogenation pathway is well understood [22,23]. Second, recent studies on ethylene hydrogenation by MoAl alloy films allow us to make a straightforward comparison between the chemistry on the alloy and the carbide and oxycarbide phases [24]. As will be shown below, drastic differences were found among these films in terms of ethylene adsorption, dissociation, hydrogenation and H–D exchange reactions.

2. Experimental

Temperature-programmed desorption (TPD) data were collected in an ultrahigh vacuum chamber operating at a base pressure of 8×10^{-11} Torr that has been described in detail elsewhere [13,17,18]. TPD spectra were collected at a heating rate of 10 or 15 K/s. The chamber was also equipped with a double-pass cylindrical mirror analyzer for collecting Auger spectra. These are typically collected using an electron beam energy of 3 keV and the first derivative spectra are obtained by numerical differentiation.

X-ray photoelectron spectra (XPS) were collected in another chamber operating at a base pressure of 2×10^{-10} Torr, which was equipped with Specs X-ray source and a double-pass cylindrical mirror analyzer. Spectra were typically collected with an Mg Kα X-ray power of 250 W and a pass energy of 50 eV. The alumina substrate was sufficiently thin that no charging effects were found and the binding energies were calibrated using the metallic Mo $3d_{5/2}$ feature (at 227.4 eV binding energy) as a standard [17,18].

The Mo(1 0 0) substrate (1 cm diameter, 0.2 mm thick) was cleaned using a standard procedure, which consisted of argon ion bombardment (2 kV, 1 μA/cm^2) and any residual contaminants were removed by briefly heating to 2000 K in vacuo. The resulting Auger spectrum showed no contaminants. Aluminum was deposited onto Mo(1 0 0) from a small heated alumina tube as described previously [13,17,18]. Alumina thin films are formed by cycles of aluminum deposition-water vapor oxidation-annealing, until the Mo(1 0 0) XPS or AES features are completely obscured. The resulting film is approximately 20 Å thick as measured using a method provided by Madden and Goodman [25].

Molybdenum hexacarbonyl (Aldrich, 99%) and ethylene (Matheson, 99.5%) were transferred to glass vials, connected to the gas-handling line of the chamber and purified by repeated freeze–pump–thaw cycles, followed by distillation, and their purities were monitored using mass spectroscopy. CO, H_2 and D_2 (Matheson, ≥99.5%) were used without further purification. These were dosed onto the surface via a capillary doser to minimize background contamination where exposures in Langmuirs ($1\,L = 1 \times 10^{-6}$ Torr s) were corrected using an enhancement factor determined using temperature-programmed desorption (see [13] for a more detailed description of this procedure).

3. Results

Fig. 1 displays a series of H_2 TPD profiles from the oxycarbide film formed using an exposure of 5000 L of $Mo(CO)_6$ to a dehydroxylated alumina thin film at 700 K, and after annealing to higher temperatures, where the annealing temperatures are marked adjacent to each desorption profile. Hydrogen was adsorbed at a sample temperature of 200 K to eliminate background CO adsorption. Neither hydrogen nor water (data not shown) desorption are detected from films annealed to 900 K, suggesting these surfaces are incapable of dissociating H_2. However, a weak yet detectable H_2 signal is observed after the film is annealed to 1000 K. Further annealing results in a drastic increase in hydrogen yield. After annealing at 1300 K (where all oxygen within the carbide film has been removed and a MoAl alloy started to form [18]), the hydrogen desorption profile peaks at ~310 K, and desorption ceases by ~550 K. When the film is annealed to 1400 K, where carbidic carbon is completely

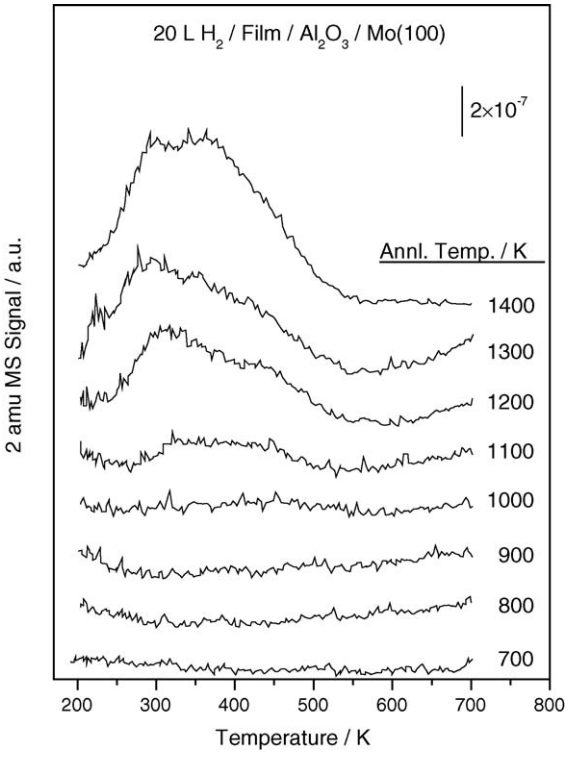

Fig. 1. The 2 amu temperature-programmed desorption spectra of hydrogen adsorbed on an oxycarbide film and on films annealed to higher temperatures. H_2 (20 L) was adsorbed at 200 K and spectra were collected at a heating rate of 10 K/s. Annealing temperatures are marked adjacent to the corresponding spectrum.

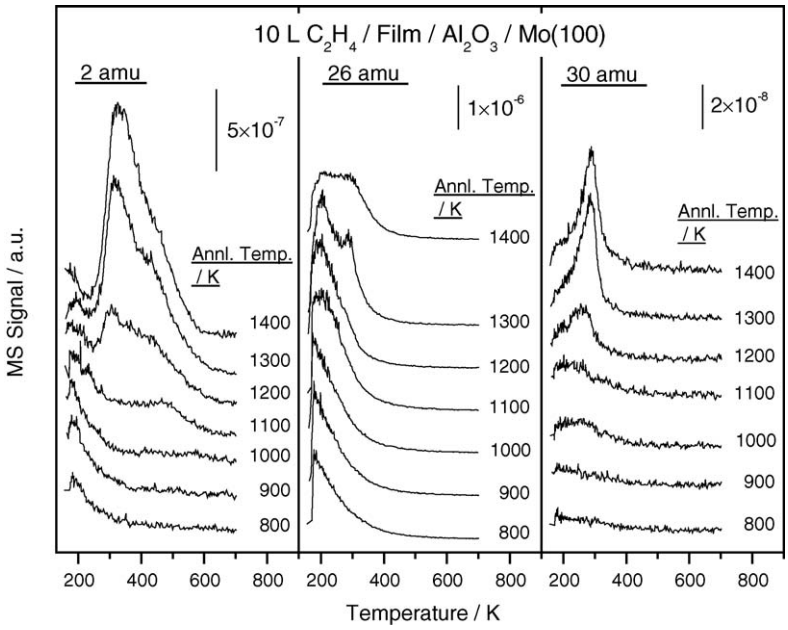

Fig. 2. The 2 amu (H_2), 26 amu (C_2H_4) and 30 amu (C_2H_6) temperature-programmed desorption spectra of ethylene adsorbed on an oxycarbide film and on films annealed to higher temperatures. Ethylene (10 L) was adsorbed at 150 K and spectra were collected at a heating rate of 10 K/s. Annealing temperatures are marked adjacent to the corresponding spectrum.

removed and the MoAl alloy is fully generated, a further increase in the hydrogen yield is found.

In order to investigate whether these surfaces are capable of catalyzing ethylene hydrogenation, a similar series of TPD experiments were performed by adsorbing 10 L of ethylene at 150 K on the oxycarbide and on surfaces that had been annealed to higher temperatures. Fig. 2 displays the resulting 2 amu (H_2), 26 amu (C_2H_4) and 30 amu (C_2H_6) desorption profiles. No H_2 desorption is found for films annealed to 800 and 900 K, suggesting that ethylene does not dissociate on these surfaces. On surfaces annealed to 1000 K, only trace amounts of H_2 are detected at 400 K and above. After annealing to 1100 K, a clear H_2 desorption state is found at ~500 K. When the film is annealed to 1200 K and above, two H_2 desorption states are found at ~300 and ~450 K respectively, the former being more intense. This indicates that ethylene decomposes on these surfaces to desorb hydrogen, the resulting carbon being deposited onto the surface as a carbide. Molecular ethylene desorbs at ~180 K for films annealed to 1000 K while on films heated to 1100 and 1200 K, the desorption temperature increased to ~195 K. Signals due to ethylene fragmentation are also detected in the 2 amu profiles. Drastic changes occur after the sample is heated to 1300 and 1400 K. In addition to a further slight temperature increase for the low-temperature ethylene state (to ~205 K), a high-temperature state is found at ~285 K. The hydrogen desorption yield increase found for the alloy surface (after the sample is annealed to1400 K) indicates substantial ethylene decomposition. These results suggest that the interaction between ethylene and the surface becomes stronger for surfaces annealed to higher temperatures. Essentially no ethane is formed on surfaces annealed to 800 and 900 K, while after annealing the film to 1000 and 1100 K, a small amount of ethane desorbs at ~235 K. The ethane yield increases for higher annealing temperatures, and the desorption temperature increases from ~260 K (for a sample annealed to 1200 K) to ~280 K (for a sample annealed to 1300 and 1400 K).

The ethane formed in these experiments is due to ethylene self-hydrogenation, where the surface hydrogen originates predominantly from the ethylene dissociation. On the alloy surface, a small portion of hydrogen is also due to adsorption from the background [24]. Since the ethane yield may be limited by the availability of surface hydrogen, experiments were therefore performed on hydrogen-precovered surfaces. Again hydrogen is adsorbed on the surfaces at 200 K at an exposure of 20 L. The results shown in Fig. 3 closely resemble the data of Fig. 2 for sample annealing temperatures below 1100 K since only a small hydrogen coverages are attained on these surfaces (Fig. 1). However, after annealing to above 1100 K, both the hydrogen and ethane yields increase dramatically compared to the clean surfaces, indicating the availability of surface hydrogen plays an important role in ethane formation, as expected.

It appears that the lack of catalytic activity for the oxycarbide film formed at 700 K is due to site blocking effects, where the as-formed film is saturated by dissociatively adsorbed CO that cannot be avoided since $Mo(CO)_6$ is used as the reactant. The fact that annealing these films to 1000 K (where CO desorption commences [18]) results in some hydrogenation activity partially supports this argument, since it is reasonable to assume that surface oxygen tends to desorb first (in the form of CO). In order to address this question, two approaches were applied to generate carbide films starting from the MoAl thin film, either using CO or ethylene as carburizing reagents.

Fig. 4(a) shows typical Auger spectra following the reaction of CO with a MoAl alloy film at 700 K. The spectra of the oxycarbide and alloy films are also displayed for direct comparison. Note that the alloy film is carbon free. Drastic changes

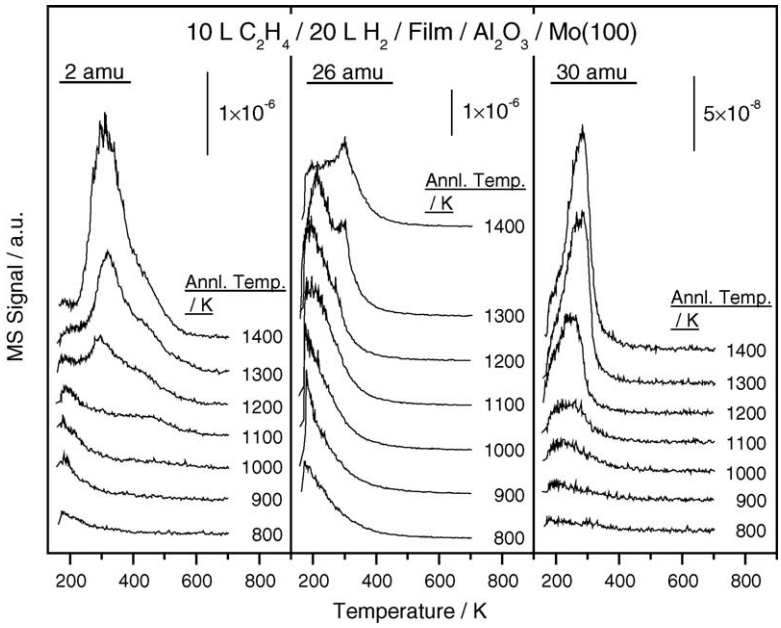

Fig. 3. The 2 amu (H_2), 26 amu (C_2H_4) and 30 amu (C_2H_6) temperature-programmed desorption spectra of ethylene adsorbed on an oxycarbide film and on films annealed to higher temperatures. Ethylene (10 L) was adsorbed at 150 K on surfaces precovered with 20 L of H_2 at 200 K and spectra were collected at a heating rate of 10 K/s. Annealing temperatures are marked adjacent to the corresponding spectrum.

occur following reaction with 20 L of CO. First, the intensity of the Al^0 signal at 66 eV decreases substantially, accompanied by an increase in the Al^{3+} (54 eV) and O (512 eV) signals. Second, a carbon signal appears at 271 eV with a lineshape that is characteristic of carbidic carbon. The Al^0 signal disappears completely following reaction with 50 L of CO. Further increasing the CO exposures to 800 L, results in further increases in the intensities of the carbon and oxygen signals. Note that carbon is carbidic at all CO exposures. Clearly a molybdenum oxycarbide film is generated, at least at high CO exposures. Fig. 4(b) plots the corresponding C/Mo peak-to-peak intensity ratios, and the resulting C/Mo stoichiometry calculated using published Auger atomic sensitivity factors for C (0.614) and Mo (1.278) [26], as a function of CO exposure. The C/Mo ratio increases rapidly for CO exposures up to 100 L, and slows down and saturates at higher exposures. The C:Mo stoichiometry saturates at ~0.6 suggesting the formation of a Mo_2C-like film. Carbon and oxygen can be easily removed as CO and the results are displayed in Fig. 4(c). At the smallest initial CO exposures, the desorption profile peaks at ~1155 K, but decreases with increasing initial CO exposures and remains constant at ~1105 K at exposures of 100 L and above. The desorption yield of this state also saturates at initial CO exposures of ~100 L. At higher exposures, a low-temperature shoulder appears in the TPD spectrum, which extends down to 800 K at the highest CO exposure.

XPS was also used to monitor the carbide film. Fig. 4(d) displays the C 1s region following the reaction of the alloy with 200 L CO at 700 K. While the initial alloy surface is essentially carbon free, an intense carbon feature is detected following reaction with CO. It should be mentioned, the C 1s binding energy of 282.5 eV suggests the presence of a carbide, consistent with the Auger results (Fig. 4(a)). Fig. 4(e) depicts the corresponding Mo 3d region before and after reaction. A Mo $3d_{5/2}$ feature is detected at ~227.1 eV for the pure alloy [17,18]. The binding energy increases to 227.4 eV after reaction, simply because aluminum has been oxidized by CO. Note that this binding energy is identical to that of pure Mo(1 0 0), suggesting that oxygen bonds preferentially to aluminum. Even at the largest CO exposure (800 L, data not plotted), no molybdenum binding energy increase was found. Note, however, that the films formed in these cases, at least at high CO exposures, are oxycarbides with surfaces that are saturated by dissociated CO. The C 1s and Mo 3d binding energies measured here are close to those found previously for MoC_x [27,28].

Ethylene hydrogenation reactions were performed on the CO-treated surfaces. Shown in Fig. 5 is a series of TPD results for ethylene self-hydrogenation where the alloy has first been reacted with various amount of CO at 700 K before cooling to 150 K, following which the surface was exposed to 5 L of ethylene. Even after the alloy surface had reacted with 1 L of CO, the H_2 yield decreased drastically. However, the surface is still capable of dissociating ethylene and forming some ethane after reaction with 20 L of CO. When the surface was reacted with 50 L of CO at 700 K, the hydrogenation activity is completely lost. Note that, at this CO exposure, no Al^0 can be detected by Auger spectroscopy. At CO exposures of 50 L and above, the hydrogenation activity can only be regained after the surface is annealed to 900 K and above (not plotted), showing identical behavior to that in Fig. 1.

The above experimental data clearly demonstrate that oxycarbide films formed at 700 K, either directly from $Mo(CO)_6$ or by reacting CO with the alloy film, is inactive for ethylene hydrogenation. As suggested by Chen et al. [29], this is mainly due to site-blocking effects by chemisorbed oxygen where these authors found that molybdenum carbides become inactive for hydrogenation after adsorbing even small amounts of O_2 at

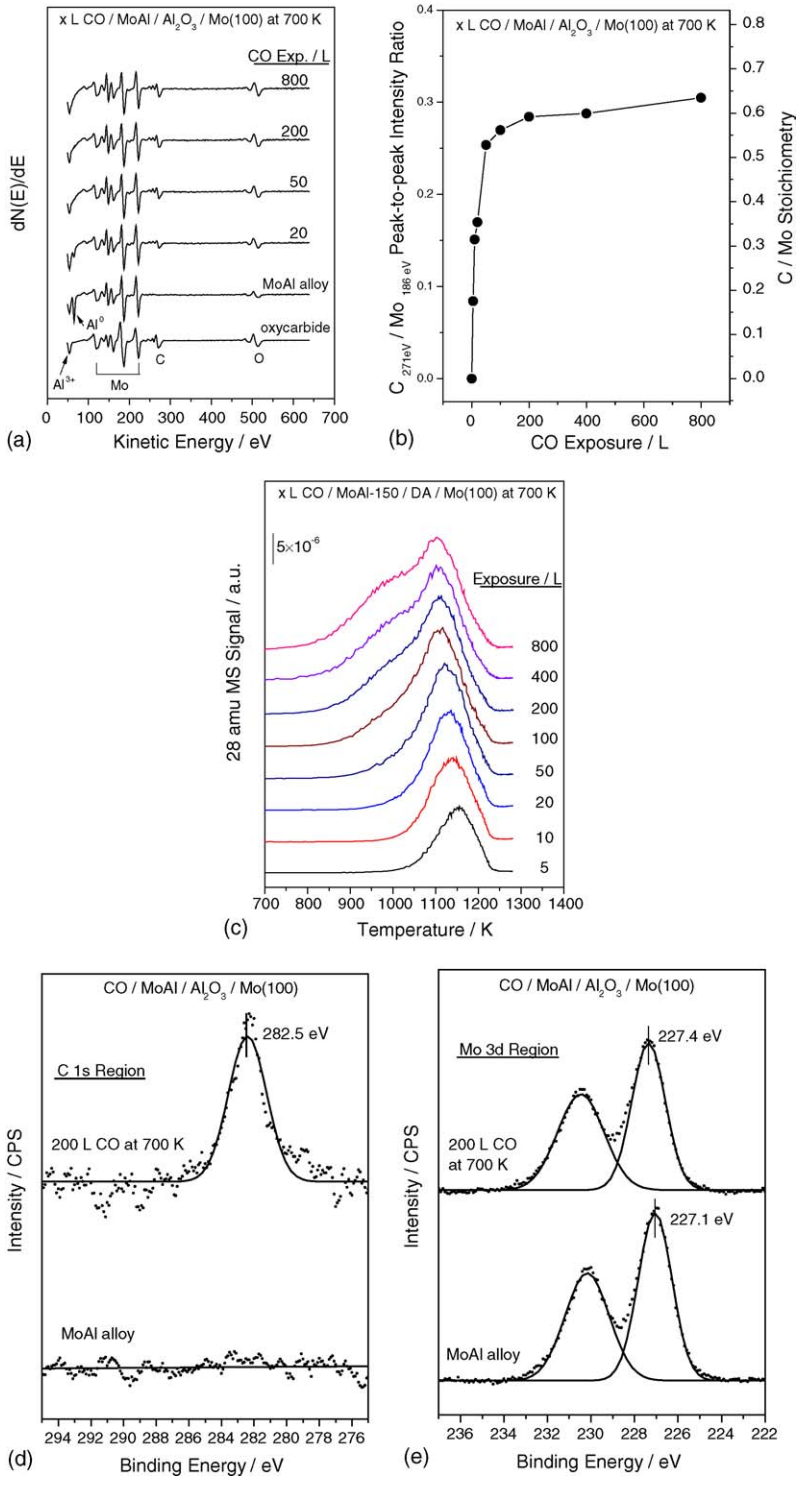

Fig. 4. Auger spectra after MoAl alloy was exposed to various amount of CO at 700 K. CO exposures are marked adjacent to the corresponding spectrum. Spectra of oxycarbide and alloy films are also displayed for comparison. All spectra were taken at room temperature. The corresponding $C_{271\,eV}/Mo_{186\,eV}$ peak-to-peak intensity ratio and stoichiometry as a function of CO exposure, taken from (a). 28 amu (CO) temperature-programmed desorption spectra of CO adsorbed on a MoAl alloy film at 700 K, as a function of CO exposure. Spectra were collected at a heating rate of 15 K/s and CO exposures are marked adjacent to the corresponding spectrum. Narrow scan X-ray photoelectron spectrum of C 1s region of 200 L of CO adsorbed on an alloy surface at 700 K. Spectrum of the alloy is also displayed for comparison. All spectra were taken at room temperature. Narrow scan X-ray photoelectron spectrum of Mo 3d region of 200 L of CO adsorbed on an alloy surface at 700 K. Spectrum of the alloy is also displayed for comparison. All spectra were taken at room temperature.

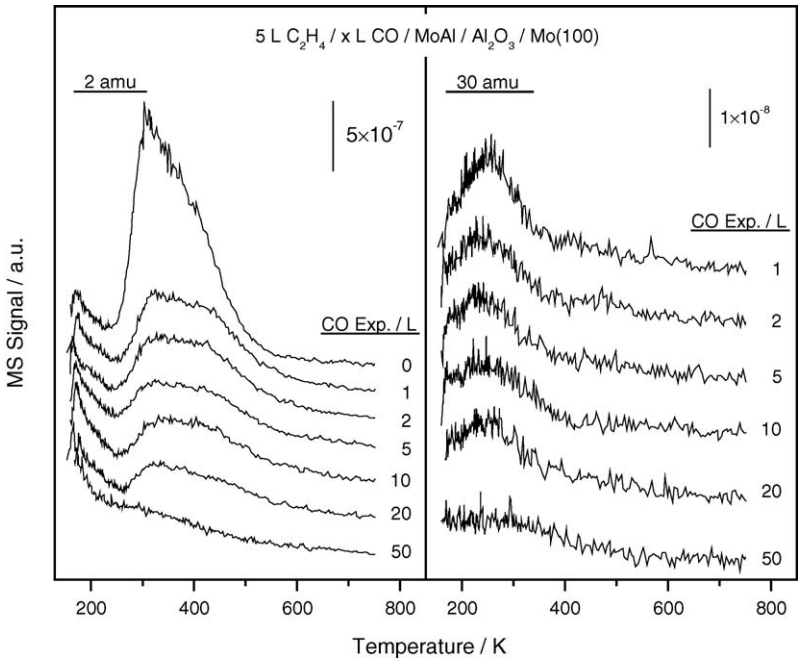

Fig. 5. The 2 amu (H_2) and 30 amu (C_2H_6) temperature-programmed desorption spectra of ethylene adsorbed on an alloy film pre-dosed with various amount of CO at 700 K. Ethylene (5 L) was adsorbed at 150 K and spectra were collected at a heating rate of 10 K/s. CO exposures are marked adjacent to the corresponding spectrum.

600 K. As suggested above, both $C_{(ads)}$ and $O_{(ads)}$ are on the surface following CO dissociation, so that it is of interest to explore whether $C_{(ads)}$ or $O_{(ads)}$ is primarily responsible for deactivation. In this case, carbide films are synthesized by reacting ethylene with an alloy film at 700 K to form an oxygen-free carbide film.

Fig. 6(a) presents a series of Auger spectra obtained following reaction with various exposures of ethylene to a MoAl alloy film at 700 K, where ethylene exposures are marked adjacent to each spectrum. The spectrum of the alloy film itself is also displayed for comparison. Apparently, carbides are formed following reaction with ethylene. In contrast to the spectra shown in Fig. 4(a), the Al^0 signal persists and the intensity of the O signal does not increase so that the only species deposited on the surface is carbon. Fig. 6(b) displays the corresponding C/Mo stoichiometry derived from the peak-to-peak intensity ratios of the $C_{271\,eV}$ and $Mo_{186\,eV}$ signals. In contrast to Fig. 4(b), in this case, MoC rather than Mo_2C is formed at the highest ethylene exposures. By analogy with data shown in Fig. 4(c), the deposited carbon can also be removed during annealing and the results are plotted in Fig. 6(c). Note that in this case, CO formation is due to the reaction between carbidic carbon and the alumina substrate. At the lowest ethylene exposures, CO desorbs at ∼1200 K, but this temperature increases gradually with increasing ethylene exposure so that at an ethylene exposure of 400 L, CO desorbs at ∼1300 K. Meanwhile, a weaker desorption state appears at ∼1200 K for ethylene exposures of 200 L and above. Shown as an inset is the corresponding CO desorption peak area plotted as a function of ethylene exposure. The similarity between this curve and the one shown in Fig. 6(b) suggests that all deposited carbon reacts, rather than diffusing to the bulk of the film during annealing.

The ethylene hydrogenation activity is monitored on carbide films formed by carburizing the MoAl alloy by various amounts of ethylene at 700 K, where ethylene exposures are marked adjacent to the corresponding spectrum (Fig. 7). This shows that the hydrogen yield decreases with increasing C/Mo ratio in the carbide films, indicating less ethylene dissociation. The line shapes and desorption temperatures of the 26 amu (ethylene) desorption profiles, on the other hand, are almost invariant. The ethane yield decreases with increasing C/Mo ratio, but all the carbide films formed at 700 K are active for ethylene hydrogenation, in contrast to oxycarbide films formed using $Mo(CO)_6$ (Fig. 2) and large exposures of CO (Fig. 5).

Fig. 8 displays TPD spectra collected at 2, 26 and 30 amu on hydrogen-precovered carbide films formed by reaction of 100 L of ethylene with the MoAl alloy at 700 K and subsequently annealed to higher temperatures, where the annealing temperatures are marked adjacent to each desorption profile. Note that the C/Mo stoichiometry of the as-formed carbide film is ∼0.6, similar to oxycarbide films formed using $Mo(CO)_6$ or large exposures of CO (Fig. 4(b)). No noticeable differences are found in terms of ethane yield and desorption temperature for surfaces annealed up to 1100 K, consistent with the data shown in Fig. 6(c) where the carbide remains on the surface at this temperature. However, on annealing to 1200 K, the hydrogen and ethane yields increase and the ethane desorption temperature also increases. On heating to 1300 K, the desorption profiles become identical to those of the alloy surface, indicating that the alloy film is fully regenerated, also consistent with the CO desorption results (Fig. 6(c)).

Note that the carbide films formed using this strategy are systemically different from “classical” carbides because of the

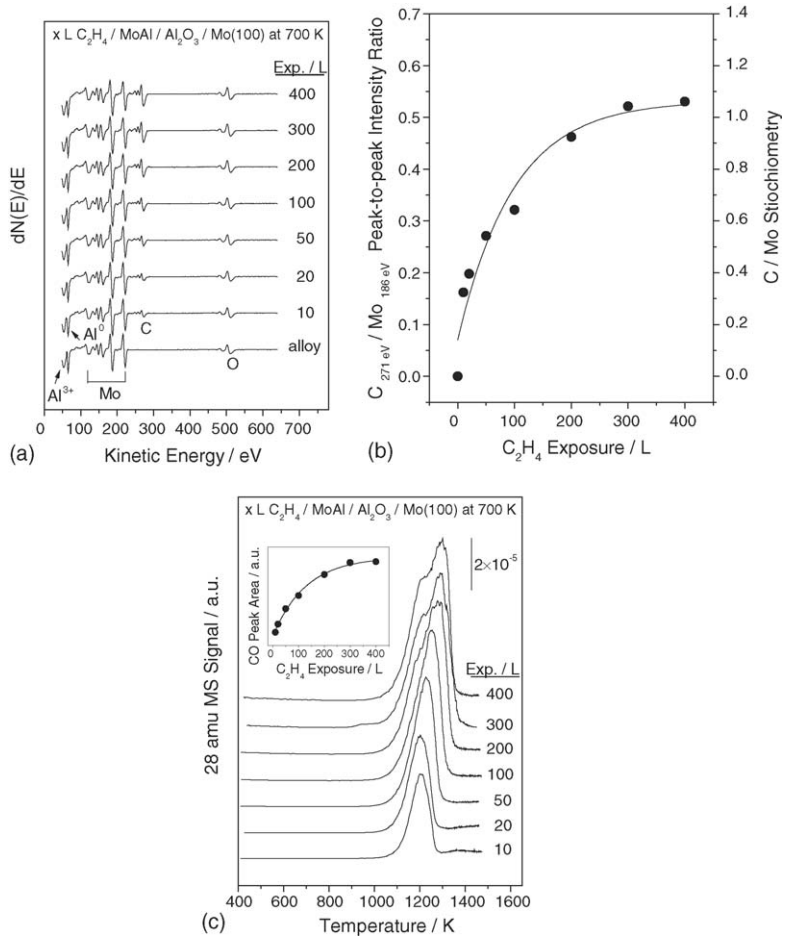

Fig. 6. Auger spectra after MoAl alloy was exposed to various amount of ethylene at 700 K. Ethylene exposures are marked adjacent to the corresponding spectrum. Spectrum of the alloy films is also displayed for comparison. All spectra were taken at room temperature. The corresponding $C_{271\,eV}/Mo_{186\,eV}$ peak-to-peak intensity ratio and stoichiometry as a function of ethylene exposure, taken from (a). 28 amu (CO) temperature-programmed desorption spectra after ethylene adsorbed on a MoAl alloy film at 700 K, as a function of ethylene exposure. Spectra were collected at a heating rate of 15 K/s and ethylene exposures are marked adjacent to the corresponding spectrum. Shown as an inset is the CO desorption area as a function of ethylene exposure.

existence of aluminum within the film. As a matter of fact, alloying with aluminum drastically changes the catalytic properties of molybdenum [24,30,31] leading to the possibility that aluminum may also modify the catalytic properties of the carbide films. Control experiments were therefore performed by using O_2 to react with the MoAl alloy at 700 K to completely oxidize metallic aluminum (monitored with Auger), and the resulting film is allowed to react with ethylene at 700 K to form a carbide. Ethylene hydrogenation reactions also occur on these carbide surfaces (data not plotted) suggesting that aluminum within the carbide film does not substantially affect the chemistry.

Finally, the H–D exchange reactions were investigated on carbide films formed from the MoAl alloy by reaction with ethylene at 700 K. In these experiments, 5 L ethylene is adsorbed onto the films precovered with 20 L of D_2. It has been shown that the MoAl alloy film catalyzes H–D exchange reactions and all the ethylene (up to C_2D_4) and ethane (up to C_2D_6) isotopomers have been detected [24]. These results are also included here for direct comparison. Fig. 9(a) displays the 2 amu (H_2), 3 amu (HD) and 4 amu (D_2) desorption profiles. The data reveal that the yields of these molecules decrease with increasing C/Mo ratio (Fig. 6(b)), consistent with data in Figs. 7 and 8. Note, however, that the desorption temperature maximum of H_2 and HD is ~310 K, while D_2 desorbs at ~290 K. This suggests that H_2 and HD formation is reaction-rate limited and that the rate-determining step is the dissociation of adsorbed ethylene or ethylene-derived hydrocarbon species. It should also be mentioned that the weak 4 amu desorption below 200 K is likely to be due to D_2 desorption from the rear of the sample or the sample holder since no HD desorbs at this temperature.

Fig. 9(b) displays the corresponding 29–32 amu desorption profiles. These have been ascribed to ethylene isotopomers C_2H_3D, $C_2H_2D_2$, C_2HD_3 and C_2D_4, respectively, on MoAl surfaces [24]. The similarity between the desorption profiles and temperatures at these masses on the carbide surfaces allows us to make the identical assignments. Note that these masses may also contain contributions from ethane isotopomers, but to a much less extent. Due to the decrease in deuterium coverage with increasing C/Mo ratio (Fig. 9(a)), the extent of H–D exchange decreases substantially. While the yield of singly exchanged product (at 29 amu, C_2H_3D) does not vary substantially with increasing C/Mo ratio, the yields of multiply exchanges

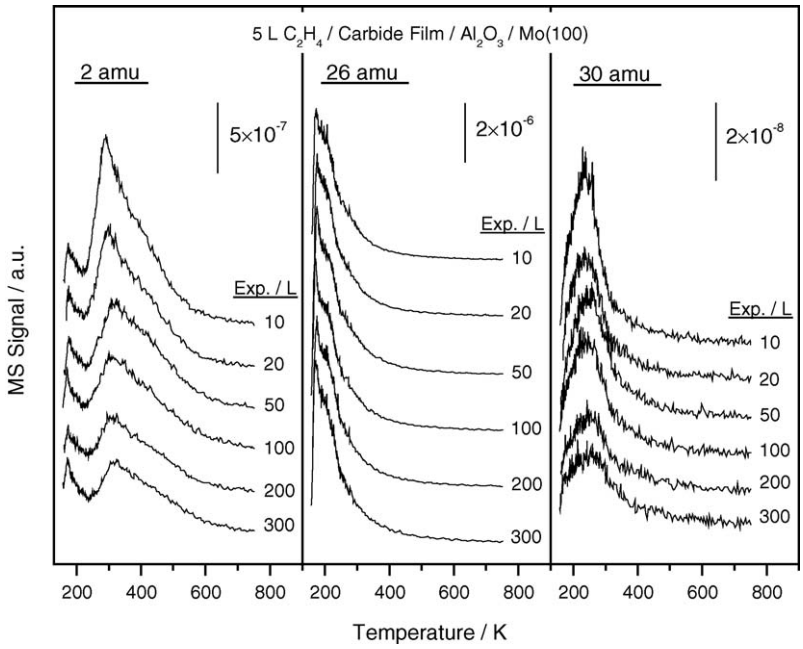

Fig. 7. The 2 amu (H_2), 26 amu (C_2H_4) and 30 amu (C_2H_6) temperature-programmed desorption spectra of ethylene adsorbed on an alloy film pre-dosed with various amount of ethylene at 700 K. Ethylene (5 L) was adsorbed at 150 K and spectra were collected at a heating rate of 10 K/s. Ethylene exposures are marked adjacent to the corresponding spectrum.

products decrease exponentially. Fig. 9(c) plots the corresponding 33–36 amu desorption profiles, which are assigned to ethane isotopomers, $C_2H_3D_3$, $C_2H_2D_4$, C_2HD_5 and C_2D_6, respectively [24]. The extent of H-D exchange also decreases rapidly with decreasing deuterium coverage so that C_2HD_5 is hardly detected when the alloy surface is treated with 20 L of ethylene at 700 K, and C_2D_6 is only formed on the alloy surface.

4. Discussion

We address first the composition of the oxycarbide, carbide and MoAl alloy films. Oxycarbide formation has been suggested to proceed, on a dehydroxylated alumina substrate, via incomplete CO disproportionation [18]. The fact that oxygen is mobile in molybdenum carbide at room temperature

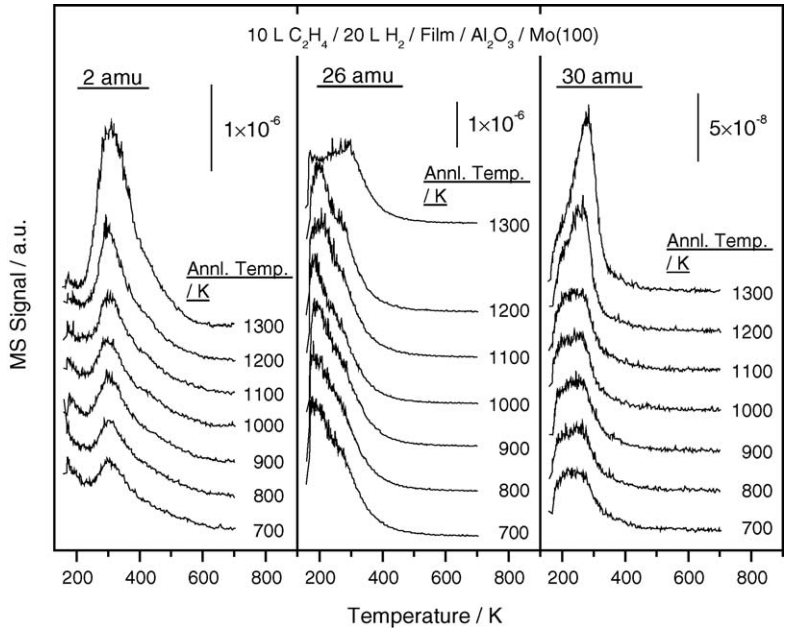

Fig. 8. The 2 amu (H_2), 26 amu (C_2H_4) and 30 amu (C_2H_6) temperature-programmed desorption spectra of ethylene adsorbed on a carbide film formed using 100 L of ethylene to react with an alloy at 700 K. Ethylene (10 L) was adsorbed at 150 K on surfaces precovered with 20 L of H_2 at 200 K and spectra were collected at a heating rate of 10 K/s. Annealing temperatures are marked adjacent to the corresponding spectrum.

and above [20,21] suggests that oxygen should be distributed throughout the whole film. It might be expected that surface oxygen deactivates the film so that it is of interest to know the oxygen content in the oxycarbide films. This was not possible, however, because of the difficulties in resolving oxygen in the film and the alumina substrate. The binding energy of molybdenum within the oxycarbide film has been found to be identical to that of pure Mo(1 0 0), suggesting that the oxygen content is rather low [18]. This is further confirmed in this study where, following H_2 adsorption on the oxycarbide films, and annealing to higher temperatures, no water formation was detected.

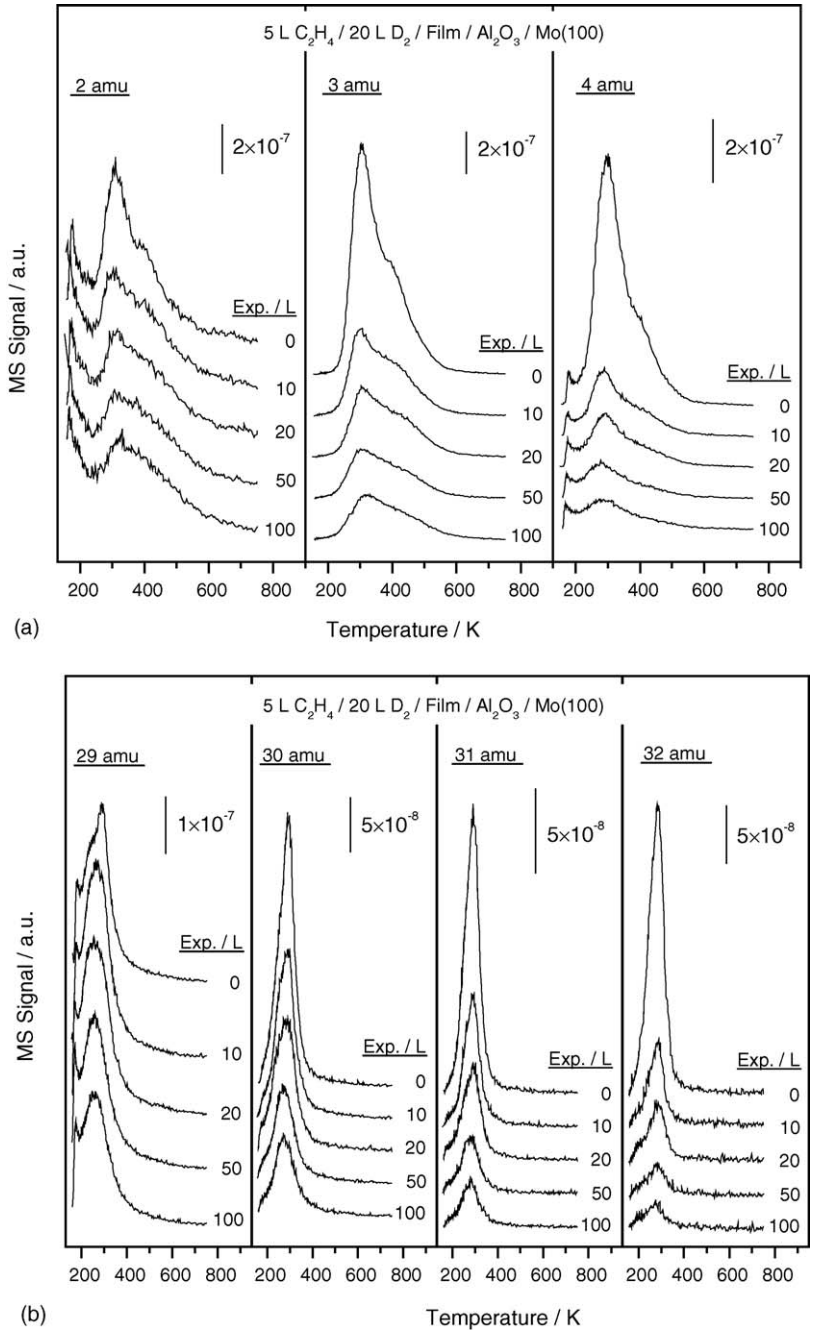

Fig. 9. The 2 amu (H_2), 3 amu (HD) and 4 amu (D_2) temperature-programmed desorption spectra of ethylene adsorbed on carbide films formed using various exposures of ethylene to react with an alloy at 700 K. Ethylene (5 L) was adsorbed at 150 K on surfaces precovered with 20 L of D_2 at 200 K and spectra were collected at a heating rate of 10 K/s. Ethylene exposures are marked adjacent to the corresponding spectrum. 29 amu (C_2H_3D), 30 amu ($C_2H_2D_2$), 31 amu (C_2HD_3) and 32 amu (C_2D_4) temperature-programmed desorption spectra of ethylene adsorbed on carbide films formed using various exposures of ethylene to react with an alloy at 700 K. Ethylene (5 L) was adsorbed at 150 K on surfaces precovered with 20 L of D_2 at 200 K and spectra were collected at a heating rate of 10 K/s. Ethylene exposures are marked adjacent to the corresponding spectrum. 33 amu ($C_2H_3D_3$), 34 amu ($C_2H_2D_4$), 35 amu (C_2HD_5) and 36 amu (C_2D_6) temperature-programmed desorption spectra of ethylene adsorbed on carbide films formed using various exposures of ethylene to react with an alloy at 700 K. Ethylene (5 L) was adsorbed at 150 K on surfaces precovered with 20 L of D_2 at 200 K and spectra were collected at a heating rate of 10 K/s. Ethylene exposures are marked adjacent to the corresponding spectrum.

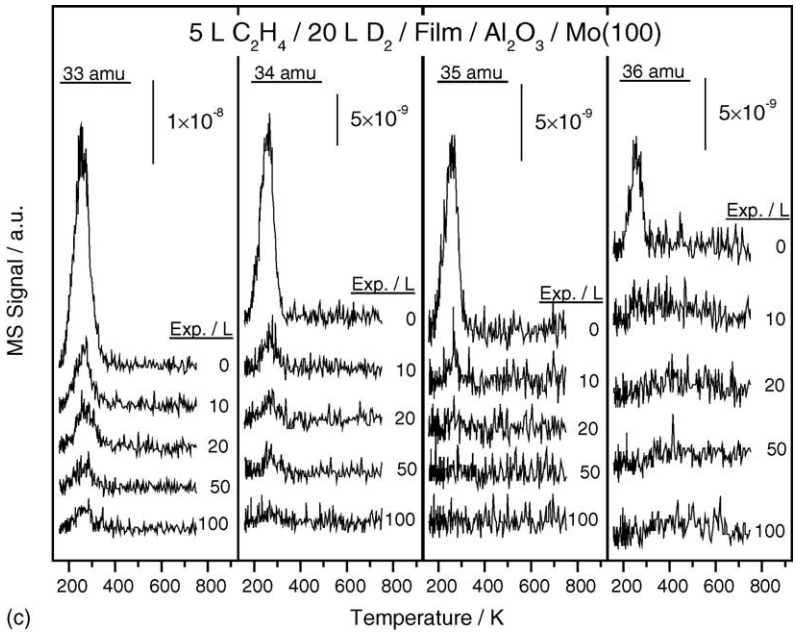

Fig. 9. (*Continued*).

Annealing the oxycarbide film formed using $Mo(CO)_6$ results in CO desorption. One would expect that the oxygen *within* the oxycarbide film would react first with carbon to form CO. This is indeed detected starting at ~1000 K at low $Mo(CO)_6$ exposures, and at ~900 K at high $Mo(CO)_6$ exposures [18]. This reaction, if it occurs exclusively, would lead to the formation of a "pure" carbide film. However, it was found, using TPD from isotopically (^{18}O) labeled alumina and by Auger spectroscopy that the alumina substrate is reduced at approximately the same temperature. At the pure carbide formation temperature (1300 K), some metallic aluminum is also generated, which diffuses into the carbide film [18]. Annealing to 1400 K removes all carbon and forms a MoAl alloy. The structure of the alloy is not well understood at an atomic level, partially because bulk molybdenum and aluminum are immiscible [32] so that no literature information is available for the bulk structure. Previous studies have shown that iodomethane and diiodomethane react with the alloy to form organoaluminum compounds [30,31]. This suggests some aluminum is located at the topmost layer of the alloy surface.

Reacting the MoAl alloy with CO and ethylene at 700 K deposits surface carbon to regenerate carbide films. In cases where CO is used as the carburizing agent, CO dissociation results in the oxidation of Al^0 at rather low CO exposures (50 L). This suggests that oxygen is bound preferentially to aluminum, consistent with the higher heat of formation of alumina compared to molybdenum oxides [33]. The data shown in Fig. 4(b) demonstrate that additional carbon is deposited after the aluminum has been fully oxidized. Again, this is due to CO disproportionation and, since this reaction does not proceed exclusively, a similar oxycarbide film will eventually form at high CO exposures. This oxycarbide appears to be different from that formed directly using $Mo(CO)_6$, since some alumina particles may be generated within the film. The saturation C/Mo stoichiometry, in these two cases, is very similar (~0.6).

The reaction of ethylene with the MoAl alloy at 700 K also results in carbide formation. In this case the carbide is oxygen-free as indicated by the constant Al^{3+} and O signals during film formation (Fig. 6(a)). Some other differences are also noticed compared with using CO as the carburizing agent. First, it is found that the C/Mo stoichiometry reaches ~1.1 (Fig. 6(b)) at the highest ethylene exposure suggesting a MoC-like film has been formed. Previous studies using similar methods, i.e. the reaction between molybdenum foils and single crystals with olefins at high temperature often forms Mo_2C-like films [34]. In that case, annealing to higher temperatures caused carbon diffusion to the molybdenum bulk. In the present study, carbon diffusion is not found because of CO formation. It is unlikely, however, that the extra carbon forms a carbidic surface layer since the MoC film is still rather active towards ethylene hydrogenation (Fig. 7).

Another difference between these films appears to be the drastic difference in CO desorption temperatures. Annealing a $Mo(CO)_6$-derived oxycarbide to 1400 K is required to remove all carbon from the surface and form the alloy [18]. In contrast, for films formed by reaction between CO and the alloy, the resulting CO desorbs at ~1150 K at the lowest exposure (Fig. 4(c)) with a desorption temperature that decreases with increasing CO exposures. On the other hand, for films formed by reaction between ethylene and the alloy, CO desorbs at ~1200 K at low ethylene exposures and increases up to ~1300 K at the highest ethylene exposure (Fig. 6(c)). It is reasonable to assume that the difference originate mainly from the availability of oxygen to react with carbidic carbon. In the first place, for films formed using $Mo(CO)_6$ on a dehydroxylated alumina substrate, although some oxygen is present *within* the oxycarbide film, and this is apparently the most reactive, extensive CO formation requires additional oxygen from the alumina substrate, which in turn needs extensive

Al–O bond cleavage and oxygen diffusion. It is also reasonable to assume that the alumina substrate is only partially reduced. In contrast to this, in cases where films are formed by reaction of CO with the alloy, small alumina particles may be located inside the carbide film facilitating their reduction. In cases where ethylene is used to form the carbide, the CO desorption temperature lies between these limits (Fig. 6(c)), presumably because the alumina substrate is more reactive, either because some alumina has been partially reduced or oxygen diffusion is more facile.

The oxycarbide films formed using $Mo(CO)_6$ (Fig. 2) and reaction of large CO exposures with the alloy (Fig. 5) at 700 K are inert towards ethylene hydrogenation. In contrast, for carbide films formed using ethylene (Fig. 7), even at the highest ethylene exposures (so that a MoC film is formed), ethylene hydrogenation is observed. This immediately suggests that the sample is deactivated by surface oxygen. This effect is due almost entirely to the fact that such surfaces are incapable of dissociating H_2 (Fig. 1), since ethylene still adsorbs on these surfaces (Fig. 2). Note that the alloy is tolerant to low exposures of CO (Fig. 5), presumably because oxygen is bound preferentially to aluminum at low coverages.

The ethane yield and desorption temperature varied gradually upon annealing the oxycarbide (Figs. 2 and 3) and carbide (Figs. 7 and 8) films. First, the oxycarbide becomes catalytically active upon annealing to 1000 K indicating some surface oxygen has been removed, consistent with TPD results (Fig. 4(c)). This is in accord with the results of Bugyi and Solymosi [35] where it was found that CO dissociates on Mo_2C at 300–350 K and recombines at 960 K and above. Second, continuous annealing results in an increased ethane yield and desorption temperature (Figs. 2 and 3). Clearly the increase in ethane yield correlates well with the increased availability of surface hydrogen (Fig. 1), and the increase in desorption temperature is controlled mainly by the strength of the interaction between ethylene and the surfaces. The 26 amu (ethylene) desorption profiles shown in Figs. 2, 3 and 8 all clearly confirm this point. On the alloy surface, ethylene desorbs in two states, one at below 200 K and another at ~285 K. These have been assigned to π- and di-σ-bonded ethylene, respectively. The σ–π parameter for the high-temperature state has been found to be ~0.8, using reflection-absorption infrared spectroscopy. It has been found that both of these ethylenic species hydrogenate to form ethane, while the desorption activation energy of π-bonded ethylene is substantially smaller than that of the di-σ form [24]. On carbide surfaces, these two ethylene desorption states are less well resolved, presumably because the weaker interaction between ethylene and the surface results in a smaller desorption temperature difference between π- and di-σ-bonded ethylene. Fruhberger and Chen [36], using high-resolution electron energy loss spectroscopy (HREELS), demonstrated that di-σ-bonded ethylene is present on carbide-modified molybdenum surfaces. However, theoretical calculations suggest that there is only a small energy difference between di-σ- and π-bonded ethylene on molybdenum carbide surfaces, and the transition state is approximately the average of the di-σ and π structures [37]. We therefore suggest that both ethylenic species are present on the carbide films and that the σ–π parameter of di-σ-bonded ethylene is lower than for the MoAl alloy.

According to the Horiuti–Polanyi mechanism [38], ethylene hydrogenation proceeds *via* an ethyl intermediate. Ethyl formation has been proposed to be slower than ethyl hydrogenation by grafting ethyl intermediates on the surface using ethyl iodide [24]. It is reasonable to argue that the stronger the interaction between ethylene and the surface, the higher the activation barrier that has to be overcome to generate this intermediate. We believe this is the reason that annealing the films to higher temperatures results in higher ethane desorption temperatures.

Extensive H–D exchange reactions occur on the alloy surface (Fig. 9). The mechanism has been proposed to involve fast ethylene–ethyl–ethylene interconversion steps [24]. It is also clear that, on the alloy, the ethylene isotopomer desorption temperature is essentially identical to that of di-σ-bonded ethylene, suggesting di-σ-, instead of π-bonded ethylene is involved in H–D exchange. The same conclusion applies to carbide surfaces (Fig. 9(b)) where it is found that the desorption temperatures of ethylene isotopomers are apparently higher than the desorption peak maximum of ethylene, but rather close to the high-temperature shoulder assigned to di-σ-bonded ethylene (Figs. 7 and 8).

5. Conclusions

Molybdenum oxycarbides are formed by reaction of $Mo(CO)_6$ with alumina films grown on a Mo(1 0 0) substrate. No hydrogen adsorbs on this surface and it is completely inactive for ethylene hydrogenation. The inactivity is ascribed to the presence of oxygen on the surface of the oxycarbide and this is confirmed by synthesizing either oxycarbides or carbides by reacting CO or ethylene respectively with a MoAl alloy. Heating the oxycarbide to above ~1100 K results in the formation of molybdenum carbide, which shows some activity for ethylene hydrogenation. Further heating to above ~1440 K results in the formation of a MoAl alloy, which is very active both for ethylene hydrogenation and H/D exchange.

Acknowledgments

We gratefully acknowledge support of this work by the Chemistry Division of the National Science Foundation under grant number CTS-0105329. One of us (YW) would like to acknowledge a dissertator fellowship from the University of Wisconsin-Milwaukee.

References

[1] A. Brenner, J. Mol. Catal. 5 (1979) 157.
[2] E. Davie, D.A. Whan, C. Kemball, J. Catal. 24 (1972) 272.
[3] J. Smith, R.F. Howe, D.A. Whan, J. Catal. 34 (1974) 191.
[4] R. Thomas, J.A. Moulijn, J. Mol. Catal. 15 (1982) 157.
[5] A. Brenner, R.L. Burwell Jr., J. Am. Chem. Soc. 97 (1975) 2565.
[6] A. Brenner, R.L. Burwell Jr., J. Catal. 52 (1978) 353.
[7] R.F. Howe, Inorg. Chem. 15 (1976) 486.
[8] A. Kazusaka, R.F. Howe, J. Mol. Catal. 9 (1980) 183.
[9] K.P. Reddy, T.L. Brown, J. Am. Chem. Soc. 117 (1995) 2845.

[10] A. Zecchina, E.E. Platero, C.O. Areán, Inorg. Chem. 27 (1988) 102.
[11] R.F. Howe, I.R. Leith, J. Chem. Soc., Faraday Trans. I 69 (1973) 1967.
[12] W.M. Shirley, B.R. McGarvey, B. Maiti, A. Brenner, A. Cichowlas, J. Mol. Catal. 29 (1985) 259.
[13] M. Kaltchev, W.T. Tysoe, J. Catal. 193 (2000) 29.
[14] M. Kaltchev, W.T. Tysoe, J. Catal. 196 (2000) 40.
[15] Y. Wang, F. Gao, M. Kaltchev, D. Stacchiola, W.T. Tysoe, Catal. Lett. 91 (2003) 83.
[16] Y. Wang, F. Gao, M. Kaltchev, W.T. Tysoe, J. Mol. Catal. A: Chem. 209 (2004) 135.
[17] Y. Wang, F. Gao, W.T. Tysoe, J. Mol. Catal. A: Chem. 236 (2005) 18.
[18] Y. Wang, F. Gao, W.T. Tysoe, J. Mol. Catal. A: Chem. 235 (2005) 173.
[19] Y. Wang, F. Gao, W.T. Tysoe, J. Mol. Catal. A: Chem., in press.
[20] K.J. Leary, J.N. Michaels, A.M. Stacy, J. Catal. 101 (1986) 301.
[21] K.J. Leary, J.N. Michaels, A.M. Stacy, J. Catal. 107 (1987) 393.
[22] F. Zaera, Chem. Rev. 95 (1995) 2651.
[23] B.E. Bent, Chem. Rev. 96 (1996) 1361.
[24] F. Gao, Y. Wang, L. Burkholder, W.T. Tysoe, Surf. Sci., in press.
[25] H.H. Madden, D.W. Goodman, Surf. Sci. 150 (1985) 39.
[26] D. Briggs, J.T. Grant (Eds.), Surface Analysis by Auger and X-ray Photoelectron Spectroscopy, IM Publications and Surface Spectra Limited, UK, 2003.
[27] B. Früberger, J.G. Chen, J. Eng, B.E. Bent, J. Vac. Sci. Technol. A 14 (1996) 1475.
[28] J.A. Rodriguez, J. Dvorak, T. Jirsak, J. Phys. Chem. B 104 (2000) 11515.
[29] H.H. Hwu, M.B. Zellner, J.G.G. Chen, J. Catal. 229 (2005) 33.
[30] Y. Wang, F. Gao, W.T. Tysoe, Surf. Sci. 590 (2005) 181.
[31] Y. Wang, F. Gao, W.T. Tysoe, J. Phys. Chem. B 109 (2005) 15497.
[32] M. Janik-Czachor, A. Wolowik, A. Szummer, K. Lublinska, S. Hofmann, K. Kraus, Electrochim. Acta 43 (1998) 875.
[33] NIST Chemistry Webbook, http://webbook.nist.gov/chemistry/.
[34] H.H. Hwu, J.G. Chen, Chem. Rev. 105 (2005) 185.
[35] L. Bugyi, F. Solymosi, J. Phys. Chem. B 105 (2001) 4337.
[36] B. Fruhberger, J.G. Chen, J. Am. Chem. Soc. 118 (1996) 11599.
[37] J.W. Yu, A.B. Anderson, Surf. Sci. 254 (1991) 320.
[38] I. Horiuti, M. Polanyi, Trans. Faraday Soc. 30 (1934) 1164.